

Vitamin B₂ Removal from Aqueous Solution Using Magnetic Nanoparticles/ Orange Peel Composite: Optimization Using Response Surface Methodology

Smiley, Erfan; Tadayon, Fariba*⁺; Sohrabi, Mahmoud Reza*⁺

Department of Chemistry, Islamic Azad University, North Tehran Branch, Tehran, IRAN

ABSTRACT: In this study, the removal of vitamin B₂ from the aqueous solution using a synthesized multi-component nano-magnetic adsorbent modified by orange peel was studied. The structure and the morphology of the prepared nanocomposite were characterized using Fourier Transform InfraRed (FT-IR), X-Ray Diffraction (XRD), Scanning Electron Microscopy (SEM), Atomic Force Microscopy (AFM), Brunauer–Emmett–Teller (BET), and Dynamic Light Scattering (DLS) techniques. The average size of the synthesized nanoparticles was 80 nm. The effect of experimental parameters such as pH, amount of adsorption, and contact time on vitamin B₂ adsorption was investigated. Response Surface Methodology (RSM) based on the Central Composite Design (CCD) was used to obtain the optimum conditions for removing vitamin B₂. Results revealed that the pH=5, adsorbent dosage of 0.4 g, and contact time of 180 min were obtained as optimum conditions. The isotherms (Langmuir, Freundlich, Temkin) and kinetic (pseudo-first-order, pseudo-second-order) studies were assessed. The data were fitted well with Langmuir ($R^2=0.9984$) with $q_{max}=53.47$ mg/g and pseudo-second-order ($R^2=0.9984$) models. The results showed that the two-component magnetic nanoparticle modified with orange peel, as an adsorbent, was suitable for the process of vitamin B₂ adsorption from the aqueous solution.

KEYWORDS: Vitamin B₂; Removal; Magnetic nanoparticles; Orange peel; Nanocomposite; Response surface methodology.

INTRODUCTION

Vitamins are one of the seven nutrients that are essential for growth and development. Thirteen vitamins are known, which have roles in human nutrition. A big family of vitamins is B-group, which includes B₁, B₂, B₃, B₅, B₆, B₈, B₉, and B₁₂. Various of B-group vitamins as coenzymes possess the main role to produce energy and they are soluble in water [1]. Riboflavin known as vitamin B₂ enters the environment from the pharmaceutical and cosmetic industries. Although vitamin B₂ is essential for

the human being, its excessive amount is dangerous for living organisms. It pollutes the water resources and easily penetrates the food chain. Fig. 1 illustrates the structure of vitamin B₂.

The presence of soluble organic materials and other B vitamins in water may cause some physical and chemical changes in their structures with the resultant health risks for the human being. Then, its removal from aquatic environments is essential [2]. Electrochemical

* To whom correspondence should be addressed.

+ E-mail: sohrabi.m46@yahoo.com & f_tadayon@iau-tnb.ac.ir
1021-9986/2022/10/3626-3637 12/\$/6.02

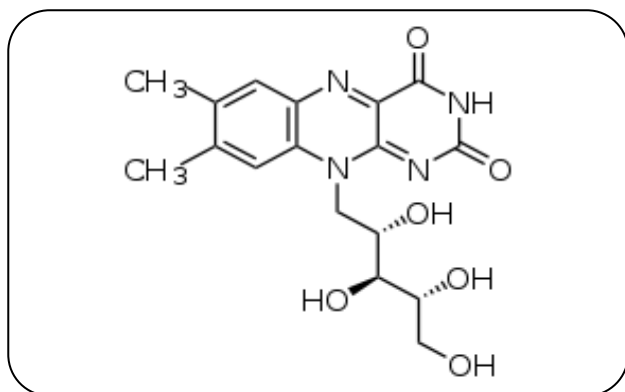


Fig. 1: Chemical structure of vitamin B₂.

stripping [3,4] and adsorption techniques [5] have been reported for the removal of vitamin B₂. Owing to simplicity, high removal performance, non-toxic by-products, and the ability to reuse, adsorption has been known as a promising procedure for the removal of contaminants from aqueous media [6,7].

In recent years, various adsorbents such as activated carbon, cellulose, and polymeric materials have been used to remove B vitamins [2]. These adsorbents have some limitations such as penetration restriction, lack of active surface sites, high cost, problems of separation from sewage and generation of secondary wastes [8-11]. *Lupaşcu et al.*, reported the adsorption of vitamin B₁₂ on highly-mesoporous activated carbons, which were obtained from lignocellulosic raw materials [12]. *Saraswat et al.*, investigated the adsorption of vitamin B₁₂ through nickel-doped, phenolic resin-based micro-nano-activated carbon adsorbents. The breakthrough analysis revealed that the VB₁₂ uptake in the bed was comparable to the equilibrium adsorption data obtained from the batch study [13]. *Aljeboree* studied the removal of vitamin B₆ from aqueous systems using ZnO. Different parameters including, initial drug concentration (5-80 mg/L), temperature (15, 25, and 50 °C), and adsorbent dosage (0.001-0.15gm) were investigated [14]. With the development of nanotechnology, nano-adsorbents such as aluminum nanoparticles, carbon nanotubes, and hydroxide-apatite nanoparticles have been used to remove pigments and vitamin B₂ in recent studies [15-17].

Aggregation of constituting units of atoms or molecules builds nanoparticles. Their size is between 1 and 100 nm. In this type of particle, the ratio of surface to volume, and the distance between energy levels are different. These two variables may induce some changes

in nanoparticle properties. In other words, by controlling the size of nanoparticles, their properties can be controlled. This process is considered a crucial step in nanoparticle synthesis [18-22].

Iron oxide nanotechnology has attracted the attention of researchers for the removal of pollutants due to its advantages such as high surface-to-volume ratio, great magnetic features, simplicity in separation, inexpensive, biocompatibility, and ability to modify its surface. However, iron oxide particles aggregate, which is a disadvantage of it. To overcome this drawback, surface modification is necessary [23]. The surface of iron oxide and nickel oxide has been modified using different materials such as cetyltrimethylammonium bromide (CTAB) [24], natural polymers [25], ionic liquid [26], activated sericite [27], etc.

Orange peel is one of the agricultural wastes produced in abundance in many countries. It is rich in pectin and other polysaccharides. Having carboxyl and hydroxyl functional groups, orange peel can be used as an adsorbent in surface adsorption processes [28,29]. It is known as a low-cost and non-toxic adsorbent, which has been used to modify the surface of nanoparticles [30]. *Ai et al.* evaluated the performance of magnetic orange peel powder biochar for the removal of ibuprofen and sulfamethoxazole from an aqueous solution. The experimental factors such as solution pH (2.0–11.0), contact time (0.5–240 min), initial drug concentration (0.5–100 mg/L), and temperatures (15–40 °C) during the removal process were assessed [31]. *Sivaraj et al.* reported the efficiency of orange peel as an adsorbent in the removal of Acid violet 17 (acid dye) from aqueous solutions. The adsorption capacity was 19.88 mg/g [32].

In the present study, for the first time, 2-component nanoparticles of iron and nickel were used to enhance the quality of nano-compounds and their effectiveness. This nanoparticle has a high surface-to-volume ratio and is easily manufactured and recycled without secondary pollution. The surface of this nanocomposite was modified by the orange peel to improve the efficiency of two-component nanoparticles for the removal of vitamin B₂ from aquatic environments. Response surface methodology based on the central composite design was applied to optimize experimental parameters, including pH, adsorbent dosage, and contact time.

EXPERIMENTAL SECTION

Materials

Iron sulfate (II) heptahydrate, nickel chloride, iron nitrate, and sodium hydroxide were obtained from Merck (Germany). The collected orange peel was washed with water and dried for 48 h at a temperature of 40°C in the oven. Then, it was crushed by a grinding mill and its fine particles of 0.1 to 0.2 mm were separated using a laboratory sieve with a mesh of 80 nm. These particles were kept in a sealed container, in a dry environment.

Apparatus and software

For morphology analysis of nanocomposite, Scanning Electron Microscopy (SEM) (SIGMA, VP-500, Zeiss, Germany) was utilized. Atomic force microscopy (AFM) (JPK instruments, Nanowizard 2) was used to study the topography of the surface. The determination of particle size distribution was performed by dynamic light scattering (DLS) (Malvern Instruments Ltd). Brunauer–Emmett–Teller (BET) (BEISORP Mini, Microtrac Bel Corp) was used to measure the specific surface area. X-ray diffraction (Panalytical, USA) and Fourier transform infrared (Perkin Elmer, USA) spectroscopy were used for the current study to further investigate the prepared nanocomposite. MINITAB 17 was used to design experiments.

Preparation of nanocomposite modified with orange peel

Eight grams of iron sulfate (II) heptahydrate, 3 g of iron nitrate (III), and 2 g of nickel chloride were simultaneously dissolved in 100 ml of distilled water and heated up to 90°C. To increase the adsorption capacity, 10 ml of 26% ammonia solution with 200 ml of a solution containing 1 g of dried and ground orange peel in distilled water was added to the initial mixture and mixed quickly. The pH of the resulting mixture was adjusted to 10 by adding 0.2 M NaOH solution and the mixture was kept at 80°C for 30 min. Finally, the mixture was cooled at room temperature and the black precipitate, which was the magnetic iron oxide attached to the orange peel, was collected by a filter paper and washed with deionized water.

Determination of removal yield

Adsorption process experiments were performed to determine parameters such as pH, contact time, and amount of adsorption. In all experiments, solutions with

a volume of 10 ml of vitamin B₂ were prepared with a certain amount of adsorbent. After the required time, the concentration of vitamin B₂ was measured. The following equations were used to calculate the removal efficiency (R%) and adsorption of vitamin B₂ (q_e) (mg/g) at equilibrium time, respectively.

$$R (\%) = \frac{(C_0 - C_e)}{C_0} \times 100 \quad (1)$$

$$q_e = \frac{(C_0 - C_e) V}{M} \quad (2)$$

Where C_0 and C_e (mg/L) are the initial concentration of the solution and residual concentration of the solution, respectively. V (L) and M (g) denote the volume of the solution and the amount of adsorbent, respectively [33].

Design of experiments

One factor at a time method is time-consuming and expensive. Thus, it is important to perform cost-effective experiments that provide the most valuable information. Design of experiments (DOE) may involve purposeful changes in inputs of a process to observe and test the changes in outputs. DOE includes an experiment or a series of experiments that consciously changes the input variables to identify the associated phenomena and to discover the realities behind the system of reactions [34-36].

In this study, the RSM was proposed to investigate the main effect of each factor, including pH, adsorbent dosage, and contact time, as well as the interaction between them. The levels of these factors were shown as +1 and -1, which represented the highest and the lowest levels, respectively. 12 experiments were designed according to this method (Table 1).

RESULTS AND DISCUSSION

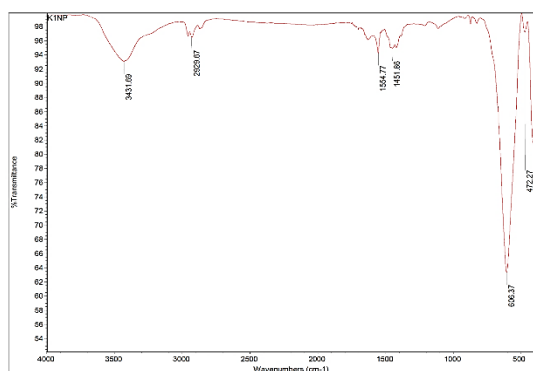
Characterization

FT-IR analysis

The FT-IR technique is the most commonly used technique to identify functional groups in organic compounds. By FT-IR spectroscopy, the two-component magnetic nanocomposite resulting from the surface adsorption method is shown in Fig. 2. The adsorption peaks indicated in the wavelength of 400-900 nm, represent the presence of iron and nickel metals, metal bonds and the formation of a two-component compound. The adsorption peaks below 1100 cm⁻¹ were related to the

Table 1: Variables, levels, and results obtained with the RSM method.

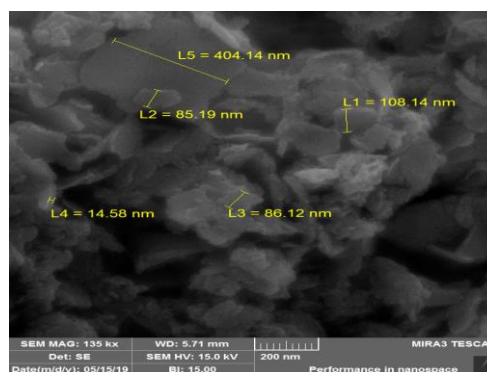
	C1	C2	C3	C4	C5	C6	C7	C8
	STD	RUN	PT	BLOCKS	pH	Time (min)	Dosage (g)	R
1	8	9	1	1	7	240	0.6	96.54
2	16	10	0	1	5	180	0.4	92.36
3	12	11	-1	1	5	180	0.4	95.44
4	13	12	-1	1	5	180	0.06	90.06
5	15	13	0	1	5	180	0.4	98.41
6	1	14	1	1	3	120	0.2	92.26
7	19	15	0	1	5	180	0.4	95.55
8	11	16	-1	1	5	80	0.4	98.22
9	3	17	1	1	3	240	0.2	93.46
10	10	18	-1	1	8	180	0.4	94.68
11	17	19	0	1	5	180	0.4	96.25
12	20	20	0	1	5	180	0.4	92.41

**Fig. 2: FT-IR spectra of a two-component magnetic nanoparticle modified with orange peel.**

the metal alloy produced. The observed peak at 3431 cm^{-1} was related to the presence of hydroxide in nanoparticles [37].

SEM analysis

The size, structure, and morphology of synthesized nanocomposite were evaluated by SEM. According to Fig. 3, this two-component compound has a dense and homogeneous surface and a suitable size. Its spherical structure led to an increase in contact surface and adsorption efficiency. The average size of the prepared particles was 139.4 nm.

**Fig. 3: SEM analysis of two-component magnetic nanoparticles modified with orange peel.**

AFM analysis

One of the most popular scanning probe microscopy approaches is AFM. Fig. 4 shows the 2D and 3D AFM results related to the prepared nanocomposite. The micrometer to nanometer scale is visible in the figure so that the dark and light colors represent the particles on the micrometer and nanometer scale, respectively.

XRD analysis

The X-ray diffraction pattern obtained from nickel and iron oxide nanoparticles modified with orange peel is shown in Fig. 5. There is no specific peak for other phases of iron

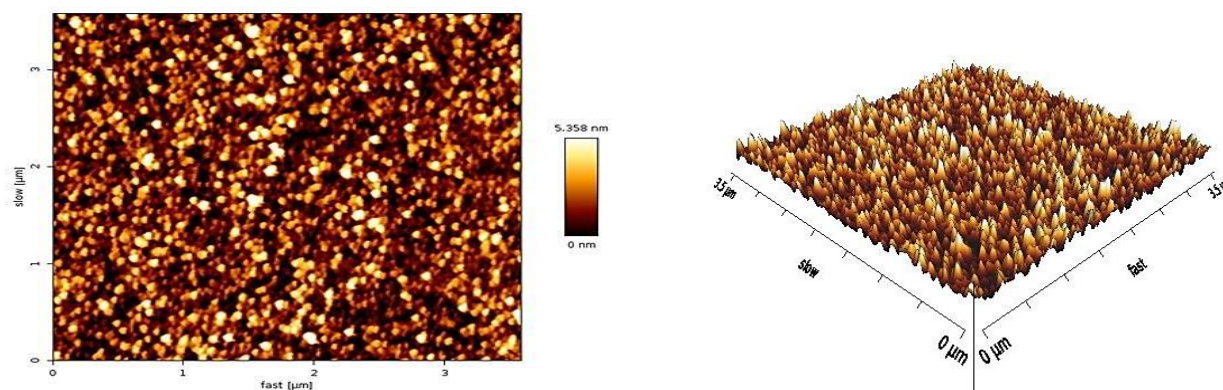


Fig. 4: 2D and 3D AFM images of two-component magnetic nanoparticles modified with orange peel.

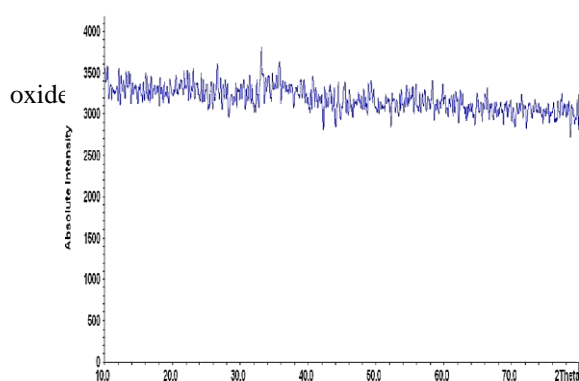


Fig. 5: XRD image of two-component magnetic nanoparticles modified by orange peel.

nanoparticles, indicating the high purity of these materials. Furthermore, there is no new peak compared to the XRD pattern of iron oxide nanoparticles, which indicated the amorphous nature of orange peel and proved the binding of iron oxide nanoparticles on orange peel. It also showed that the width of peaks increased and their intensity decreased because the nanoparticles gradually lost their crystalline state after binding the orange peel.

BET analysis

Fig. 6 exhibits the N_2 adsorption–desorption isotherm related to the two-component magnetic nanoparticles modified by orange peel. The closeness of BET theory to the Langmuir theory has been reported, which determines the specific surface area (SSA). The assumption of this theory is defined as that all layers are in equilibrium in the adsorption of the multilayer. The BET model is expressed using Eq (3).

$$\frac{P/P_0}{n(1 - \frac{P}{P_0})} = \frac{1}{n_m C} + \frac{C-1}{n_m C} (P/P_0) \quad (3)$$

Where n and n_m are a certain amount of the adsorbed gas at the relative pressure P/P_0 and the capacity of the monolayer corresponding to the adsorbed gas, respectively. P , P_0 , and C denote the pressure, the saturation pressure of a substance being adsorbed at the adsorption temperature, and BET constant, respectively [38].

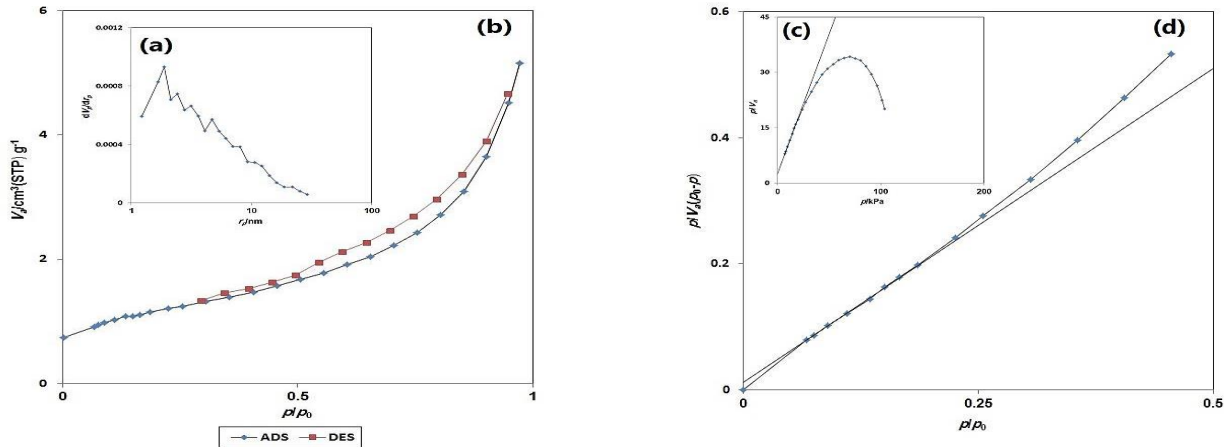
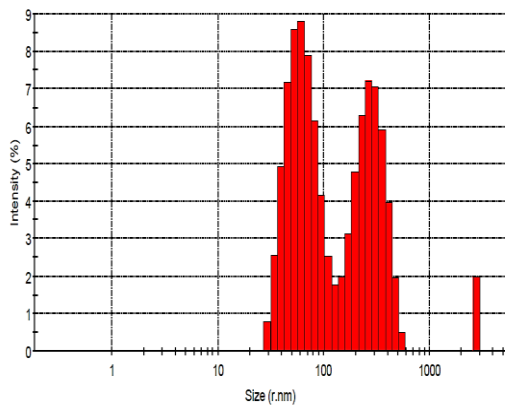
The estimation of the pore size distribution of the nanocomposite was accomplished through the Barrett-Joyner-Halenda (BJH) method (Fig. 6a). The mean volume values corresponding to the pores (V_p) and the surface of the pores (a_p) were found at $0.0072 \text{ cm}^3/\text{g}$ and $3.135 \text{ m}^2/\text{g}$, respectively. Also, $r_{p,peak}$ (Area) was achieved 1.88 nm . As shown in Fig. 6 (d), the BET plot can estimate the BET surface area with R^2 equal to 1. The values of the specific BET surface area ($a_{s,BET}$) and mean pore diameter were found to be $4.317 \text{ m}^2/\text{g}$ and 7.39 nm , respectively. BET monolayer capacity (V_m) and C were obtained at $0.9918 \text{ cm}^3/\text{g}$ and 89.01 , respectively. The Langmuir isotherm parameters (Fig. 6c), including $a_{s,Lang}$, V_m , and R^2 were obtained $5.747 \text{ m}^2/\text{g}$, $1.320 \text{ cm}^3 \text{ (STP) g}^{-1}$, 0.9993 , respectively. Table 2 represents the obtained data related to the BET and BJH.

DLS analysis

The particle size distribution was determined using the DLS technique. The results represent that the average size is 136.5 nm (Fig. 7), which is close to the average results obtained from SEM.

Table 2: The data obtained from BET and BJH methods for the two-component magnetic nanoparticles modified by orange peel.

Parameters	Nanocomposite
$a_{s,BET}$ (m ² /g)	4.317
d_0 (nm)	7.393
V_p (cm ³ /g)	0.0072
a_p (m ² /g)	3.135
V_{total} (cm ³ /g)	0.0079

**Fig. 6:** (a) the pore size distribution curve, (b) nitrogen adsorption–desorption isotherm, (c) Langmuir isotherm and (d) BET plot of nanocomposite**Fig. 7:** Particle size distributions of synthesized nanocomposite.

Optimization

The effect of pH

In general, the pH of the solution plays a major role in adsorption and adsorption capacity. In fact, since H⁺ and OH⁻ ions are highly adsorbed on the surface, they can change the adsorbent surface load, affect the ionization level of materials available in solution and separate the

functional groups in the active adsorbent sites. The effect of pH on vitamin B₂ adsorption was done using modified nanocomposite. The rate of vitamin B₂ removal by the adsorbent, which is modified by an orange peel is higher than that of an unmodified one in all pH ranges. By increasing the pH, the adsorption rate decreases. Vitamin B₂ in an aqueous solution transforms into anions. As pH decreases, the adsorbent surface is protonated, resulting in increased anionic vitamin B₂ adsorption. By increasing the pH, the solution becomes less acidic, and the negative charge density on the adsorbent surface increase. The maximum removal of vitamin B₂ was around 5. So, it was selected as the optimum pH.

The effect of adsorbent dosage

The effect of the adsorbent dosage on the adsorption of vitamin B₂ was tested in a certain volume and pH of 5 in 30 min at room temperature. By increasing the surface area, the number of adsorption sites increases. Consequently, the adsorption efficiency will be increased. In this study, according to the specified time and different

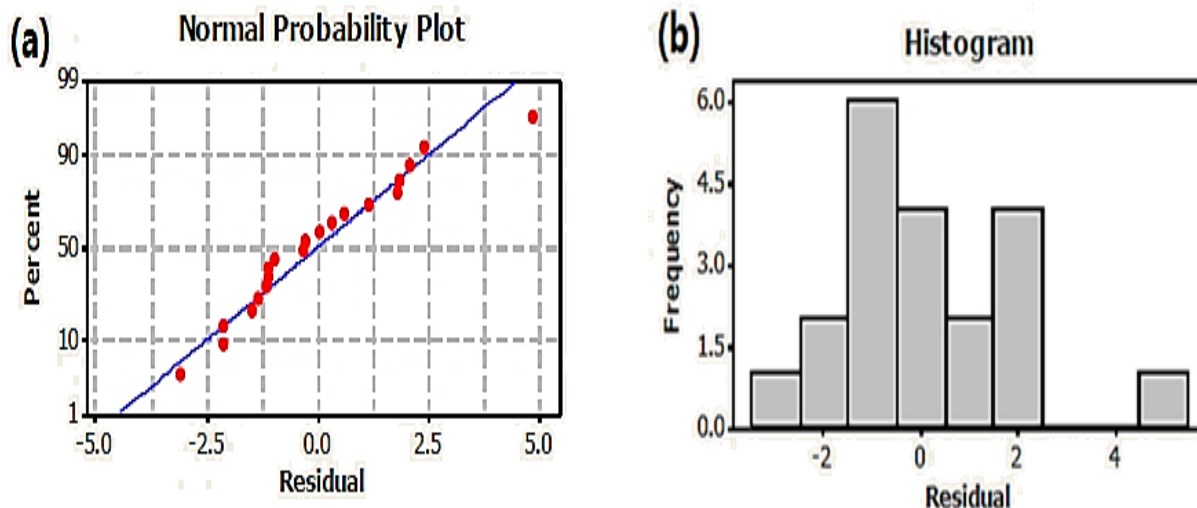


Fig. 8: (a) Normal probability and (b) histogram for removal efficiency by synthesized nanoparticles.

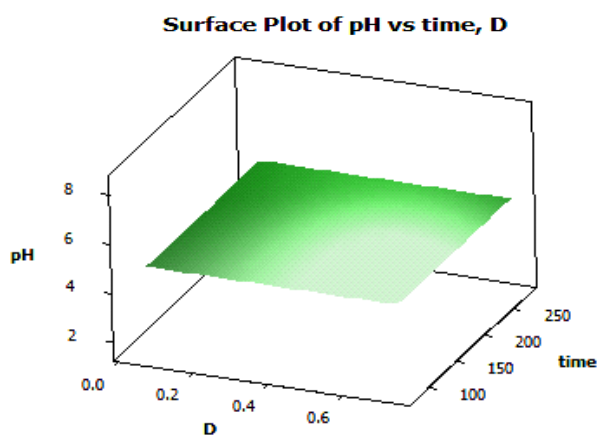


Fig. 9: Three-dimensional diagram of the effect of parameters on the size of magnetic nanoparticles.

amounts of adsorbent, the adsorption of vitamin B₂ increased with increasing the amount of adsorbent. It could be attributed to the increase in the surface area of the adsorbent and the availability of adsorption sites. By increasing the dosage of nanocomposite from 0.1 to 0.7 g, the adsorption efficiency increased. More than 0.7 g of nanocomposite did not affect the removal efficiency. This could be due to the overlap of the adsorption sites following the use of more amounts of adsorbent. The optimal adsorbent dosage for vitamin B₂ adsorption was about 0.6 g.

The effect of contact time

The adsorption of vitamin B₂ on synthesized nanocomposite was studied by varying the time (80–240 min).

By increasing the contact time until 180 min, the adsorption of vitamin B₂ was increased.

Results OF RSM

Model fitting

Fig. 8 (a) exhibited the normal probability plot of residuals, which showed the normal distribution of data. The plot of histogram is indicated that this model has well Gaussian state (Fig. 8b).

Three-dimensional response surface plots

According to the three-dimensional diagram in Fig. 9, the interaction of the parameters and their effects on the desired response can be observed. In this figure, the best results of vitamin B₂ removal were obtained at the contact time of 180 min, the adsorption dose of 0.4, and the pH of 5.

ADSORPTION ISOTHERMS

In order to achieve the adsorption isotherm, the Langmuir, Freundlich, and Temkin models were used. Surface homogeneity in terms of energy, as well as a monolayer surface coverage without interaction between the adsorbed molecules is observed [39]. The linearized equation of the Langmuir model is expressed in Eq (4).

$$\frac{C_e}{q_e} = \frac{1}{q_m K_L} + \frac{1}{q_m} C_e \quad (4)$$

Where C_e (mg/L) and q_e (mg/g) denote the drug concentration and the amount of drug adsorbed at equilibrium state, respectively. The maximum adsorption capacity and Langmuir constant of adsorption capacity are

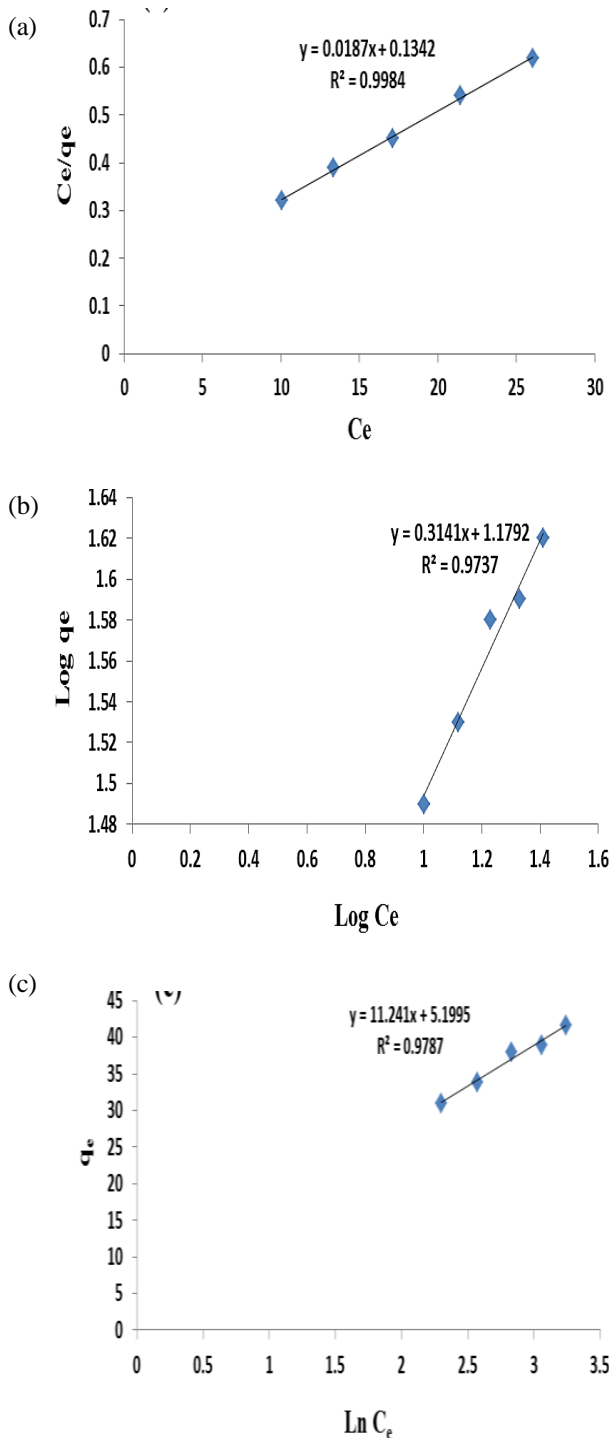


Fig. 10: (a) Langmuir, (b) Freundlich, and (c) Temkin isotherms for the removal of vitamin B₂ by synthesized NPs.

demonstrated using q_m (mg/g) and K_L (L/mg), respectively. The plot of C_e/q_e against C_e gives the values of q_m and K_L using intercept and slope of the straight line of this plot, respectively (Fig. 10a) [40].

The Freundlich model is reliable for heterogeneous surfaces that the linear form of this isotherm can be written as follows:

$$\text{Log } q_e = \log (K_f) + \frac{1}{n} \log (C_e) \quad (5)$$

The adsorption capacity (K_f) and adsorption intensity ($1/n$) are obtained via slope and intercept related to the plot of $\log q_e$ versus $\log C_e$, respectively (Fig. 10b) [41].

The Temkin isotherm is described as follows:

$$q_e = B \ln(A_T) + B \ln(C_e) \quad (6)$$

By plotting q_e versus $\ln C_e$ (Fig. 10c), Temkin constants, including B (RT/b) and A_T ($RT \ln K_T/b$) are calculated from the slope and intercept. R is the universal gas constant (8.314 J/K mol) and T is the temperature (K) [42,43].

The parameters related to these isotherms were calculated and are given in Table 3. According to the maximum coefficient of determination (R^2), the removal process follows the Langmuir isotherm with $R^2=0.9984$. The maximum adsorption capacity was obtained at 53.47 mg/g.

Adsorption kinetics

The pseudo-first-order kinetic model of drug adsorption is presented by the following equation.

$$\ln (q_e - q_t) = \ln q_e - k_1(t) \quad (7)$$

Herein q_t is the amount of drug adsorbed (mg/g) at time t . Also, the first-order kinetic constant (k_1) and amounts of drug adsorbed (mg/g) at equilibrium (q_e) were calculated by plotting $\ln (q_e - q_t)$ versus t through the slope and intercept, respectively (Fig. 11a) [44].

The equation of pseudo-second-order model is given as follows:

$$\frac{t}{q_t} = \frac{1}{k_2 q_e^2} + \frac{t}{q_e} \quad (8)$$

The second-order kinetic constant (k_2) and q_e^{cal} can be calculated experimentally from the slope and intercept related to the plot of t/q_t versus t , respectively (Fig. 11b) [45,46].

The kinetic parameters of the vitamin B₂ adsorption are summarized in Table 4. The adsorption process is in agreement with the pseudo-second-order model ($R^2=0.9984$) and $q_e=169.49$ mg/g.

Table 3: The obtained parameters of isotherm models for vitamin B₂ removal.

Langmuir			Freundlich			Temkin		
q _{max} (mg/g)	K _L (L/mg)	R ²	K _f	1/n	R ²	A _T (1/mg)	b _T (J/mol)	R ²
53.47	0.139	0.9984	15.10	0.3141	0.9737	220.40	2710.46	0.9787

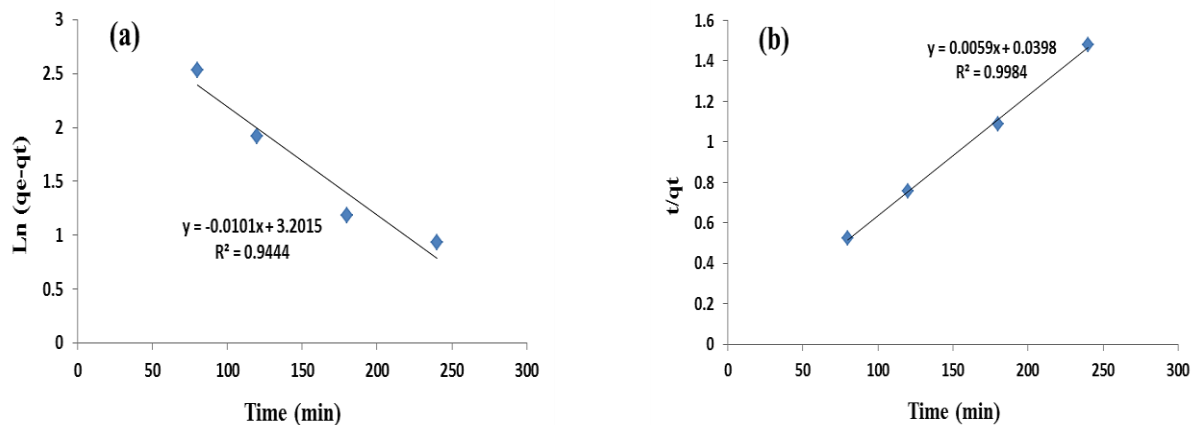
Table 4: The obtained kinetic parameters for vitamin B₂ removal.

pseudo-first order			Pseudo-second order		
K ₁ (min ⁻¹)	q _e (mg/g)	R ²	K ₂ (g/mg. min)	q _e (mg/g)	R ²
0.0101	24.56	0.9444	8.74×10 ⁻⁴	169.49	0.9984

Table 5: Comparison of the proposed adsorbent with other adsorbents.

Adsorbent	Removal efficiency (%)	Adsorption capacity (mg/g)	Pollutant	Ref.
Activated Carbon	70.00	---	Ascorbic	[47]
DUT-67 ^a	---	110.2	acid	[48]
Magnetically activated carbon	65.00	23.28	Niacin	[49]
Magnetic nanoparticles/orange peel	98.41	---	Nicotinic acid Riboflavin	Present study

^a zirconium-based metal-organic framework

**Fig. 11: (a) Pseudo first-order and (b) Pseudo second-order adsorption kinetics of adsorption process.**

A comparison with other adsorbents

The removal percentage of the proposed nanocomposite was compared with other adsorbents. The results are given in Table 5. As can be seen, the magnetic nanoparticles/orange peel has excellent removal efficiency than the other adsorbent. This adsorbent shows comparable performance.

CONCLUSIONS

In this study, the adsorption of vitamin B₂ was investigated by a two-component magnetic nanoparticle,

modified with orange peel. The optimization of important experimental parameters such as pH and adsorbent dosage and contact time was performed using RSM based on CCD. Maximum removal was achieved 98.41% in pH=5, adsorbent dosage of 0.4 g and contact time of 180 min. The Langmuir isotherm and pseudo-second-order kinetic were suitable for vitamin B₂ removal. This study indicated that the synthesized nanocomposite with useful properties such as high efficiency, inexpensive, and environmentally friendly could be an efficient adsorbent

for the removal of pharmaceuticals from aqueous solutions.

Received: May. 1, 2022 ; Accepted: Sep. 19, 2022

REFERENCES

- [1] Zhang Y., Zhou W., Yan J.Q., Liu M., Zhou Y., Shen X., Ma Y.L., Feng X., Yang J., Li G.H., [A Review of the Extraction and Determination Methods of Thirteen Essential Vitamins to the Human Body: An Update from 2010](#), *Molecules*, **23**: 1484 (2018).
- [2] Sevgi K., [Adsorption of Cd\(II\), Cr\(III\) and Mn\(II\) on natural sepiolite](#), *Desalination*, **244**: 24-30 (2009).
- [3] Yamashita M., Rosatto S.S., Kubota L.T., [Electrochemical Comparative Study of Riboflavin, FMN and FAD Immobilized on the Silica Gel Modified with Zirconium Oxide](#), *Braz. J. Chem. Soc.*, **13**: 635-641 (2002).
- [4] Sawamoto H., [Anodic and Cathodic Adsorption Stripping Analysis of Riboflavin](#), *Journal of Electroanalytical Chemistry and Interfacial Electrochemistry*, **186**: 257-265 (1985).
- [5] Mohd Din A.T., Ahmad M.A., Hameed B.H., [Riboflavin Adsorption onto Multi-Modal Mesoporous Carbon Synthesized from Polyethylene Glycol 400](#), *Chemical Engineering Journal*, **215–216**: 297–305 (2013).
- [6] Dehghani M.H., Kamalian S., Shayeghi M., Yousefi M., Heidarinejad Z., Agarwal S., Kumar Gupta V., [High-Performance Removal of Diazinon Pesticide from Water Using Multi-Walled Carbon Nanotubes](#), *Microchemical Journal*, **145**: 486-491 (2019).
- [7] Mirsoleimani-azizi S.M., Setoodeh P., Samimi F., Shadmehr J., Hamedi N., Rahimpour M.R., [Diazinon Removal From Aqueous Media by Mesoporous MIL-101\(Cr\) in a Continuous Fixed-Bed System](#), *Journal of Environmental Chemical Engineering*, **6**: 4653-4664 (2018).
- [8] Adeyemo A.A., Adeoye I.O., Solomon Bello O., [Adsorption of Dyes Using Different Types of Clay: A Review](#), *Appl Water Sci.*, **7**: 543–568 (2017).
- [9] Abd El-Latif M.M., El-Kady M.F., Ibrahim A.M., Ossman, M.E., [Alginate/ Polyvinyl Alcohol - Kaolin Composite for Removal of Methylene Blue from Aqueous Solution in a Batch Stirred Tank](#), *Reactor Journal of American Science.*, **6**: 280-292 (2010).
- [10] Wong K.K., Lee C.K., Low K.S., Haron M.J., [Removal of Cu and Pb by Tartaric Acid Modified Rice Husk from Aqueous Solutions](#), *Chemospher*, **50**: 23-30 (2003).
- [11] Srivastava V., Weng C.H., Singh V.K., Sharma Y.C., [Adsorption of Nickel Ions from Aqueous Solutions by Nano Alumina: Kinetic, Mass Transfer, and Equilibrium Studies](#), *J. Chem. Eng.*, **56**: 1414–1422 (2011).
- [12] Lupascu T., Petuhov O., Tîmbaliuc N., Cibotaru S., Rotaru A., [Adsorption Capacity of Vitamin B12 and Creatinine on Highly-Mesoporous Activated Carbons Obtained from Lignocellulosic Raw Materials](#), *Molecules*, **25**: 3095 (2020).
- [13] Saraswat R., Talreja N., Deva D., Sankararamakrishnan N., Sharma A., Verma N., [Development of Novel in Situ Nickel-Doped, Phenolic Resin-Based Micro–Nano-Activated Carbon Adsorbents for the Removal of Vitamin B-12](#), *Chemical Engineering Journal*, **197**: 250–260 (2012).
- [14] Aljeboree A.M., [Removal of Vitamin B6 \(Pyridoxine\) Antibiotics Pharmaceuticals from Aqueous Systems By ZnO](#), *International Journal of Drug Delivery Technology*, **9**: 2 (2019).
- [15] Gupta V. K., Agarwal S., Saleh T.A., [Synthesis and Characterization of Alumina-Coated Carbon Nanotubes and their Application for Lead Removal](#), *J Hazard Mater*, **185**: 17-23(2011).
- [16] Feng Y., Gong J.L., Zeng G.M., Niu Q.Y., Zhang H.Y., Niu C.G., Deng J.H., Yan M., [Adsorption of Cd \(II\) and Zn \(II\) from Aqueous Solutions Using Magnetic Hydroxyapatite Nanoparticles as Adsorbents](#), *J. Chem. Eng.*, **162**: 487-494 (2010).
- [17] Samarghandi M.R., Nouri J., Mesdaghinia A.R., Mahvi A., [Efficiency Removal of Phenol, Lead and Cadmium by Means of UV/TiO₂/H₂O₂ Processes](#), *J. Environ. Sci. Tech.*, **4**: 19-25 (2007).
- [18] Munagapati V.S., Yarramuthi V., Kim Y., Min Lee K., Kim D.S., [Removal of Anionic Dyes \(Reactive Black 5 and Congo Red\) from Aqueous Solutions Using Banana Peel Powder as an Adsorbent](#), *J Ecotox Environ Safety*, **148**: 601-607 (2018).
- [19] Munagapati V.S., Kim D.S., [Adsorption of Anionic Azo Dye Congo Red from Aqueous Solution by Cationic Modified Orange Peel Powder](#), *J. Molecular Liquids.*, **220**: 540-548 (2016).

- [20] Jung K.W., Choi B.H., Hwang M.J., Choi J.W., Lee S., Chang J.S., Ahn K.H., [Adsorptive Removal of Anionic Azo Dye from Aqueous Solution Using Activated Carbon Derived from Extracted Coffee Residues](#), *J. Cleaner Production*, **166**: 360-368 (2017).
- [21] Banerjee S., Chattopadhyay M.C., [Adsorption Characteristics for the Removal of a Toxic Dye, Tartrazine from Aqueous Solutions by a Low Cost Agricultural by-Product](#), *Arabian J. Chem.*, **10**: S1629-S1638 (2017).
- [22] Liu J.F., Zhao Z.S., Jiang G.B., [Coating Fe₃O₄ Magnetic Nanoparticles with Humic Acid for High Efficient Removal of Heavy Metals in Water](#), *J. Environ. Sci. Tech.*, **42**: 6949–6954 (2008).
- [23] Jain M., Yadav M., Kohout T., Lahtinen M., Kumar Garg V., Sillanpaa M., [Development of Iron Oxide/Activated Carbon Nanoparticle Composite for the Removal of Cr\(VI\), Cu\(II\) and Cd\(II\) Ions from Aqueous Solution](#), *Water Resources and Industry*, **20**: 54-74 (2018).
- [24] Zargar B., Parham H., Hatamie A., [Fast Removal and Recovery of Amaranth By Modified Iron Oxide Magnetic Nanoparticles](#), *Chemosphere*, **76**: 554–557 (2009).
- [25] Sharaf El-Deen G.E., Imam N.G., Ayoub R.R., [Preparation, Characterization and Application of Superparamagnetic Iron Oxide Nanoparticles Modified With Natural Polymers for Removal of ⁶⁰Co-Radionuclides from Aqueous Solution](#), *Radiochimica Acta*, **105**: 141–159 (2016).
- [26] Pillai P., Dharaskar S., Kumar Sinha M., Sillanpaa M., Khalid M., [Iron Oxide Nanoparticles Modified with Ionic Liquid as an Efficient Adsorbent for Fluoride Removal from Groundwater](#), *Environmental Technology & Innovation*, **19**: 100842 (2020).
- [27] Hidayah Abdullah N., Shameli K., Chan Abdullah E., Chuah Abdullah L., [Low Cost and Efficient Synthesis of Magnetic Iron Oxide/Activated Sericite Nanocomposites for Rapid Removal of Methylene Blue and Crystal Violet Dyes](#), *Materials Characterization*, **163**: 110275 (2020).
- [28] Zhu C., Wang L., Kong L., Yang X., Wang L., Zheng S., Chen F., Maizhi F., Zong H., [Photocatalytic Degradation of AZO Dyes by Supported TiO₂+UV in Aqueous Solution](#), *Chemosphere*, **41**: 303-309 (2000).
- [29] Sud D., Mahajan G., Kaur M., [Agricultural Waste Material as Potential Adsorbent for Sequestering Heavy Metal Ions from Aqueous Solutions – A Review](#), *Bioresour. Technol.*, **99**: 6017–6027 (2008).
- [30] Gupta V.K., Nayak A., [Cadmium Removal and Recovery from Aqueous Solutions by Novel Adsorbents Prepared from Orange Peel and Fe₂O₃ Nanoparticles](#), *Chemical Engineering Journal*, **180**: 81-90 (2012).
- [31] Ai T., Jiang X., Zhong Z., Li D., Dai S., [Methanol-Modified Ultra-Fine Magnetic Orange Peel Powder Biochar as an Effective Adsorbent for Removal of Ibuprofen and Sulfamethoxazole from Water](#), *Adsorption Science & Technology*, **38**: 304-321 (2020).
- [32] Sivaraj R., Namasivayam C., Kadirvelu K., [Orange Peel as an Adsorbent in the Removal of Acid Violet 17 \(Acid Dye\) from Aqueous Solutions](#), *Waste Management*, **21**: 105-110 (2001).
- [33] Bayat M., Alighardashi A., Sadeghasadi A., [Fixed-Bed Column and Batch Reactors Performance in Removal of Diazinon Pesticide from Aqueous Solutions By Using Walnut Shell-Modified Activated Carbon](#), *Environmental Technology & Innovation*, **12**: 148-159 (2018).
- [34] Kim J.E., Shin J.Y., Cho M.H., [Magnetic Nanoparticles: An Update of Application for Drug Delivery and Possible Toxic Effects](#), *Archives of Toxicology*, **86**: (2012) 685-700.
- [35] Polowczyk I., Kozlecki T., [Central Composite Design Application in Oil Agglomeration of Talc](#), *Physicochemical Problems of Mineral Processing*, **53**: 1061–1078 (2017).
- [36] Yiew Ooi T., Ling Yong E., Fadhil Md Din M., [Optimization of Aluminium Recovery from Water Treatment Sludge Using Response Surface Methodology](#), *Journal of Environmental Management*, **228**: 13-19 (2018).
- [37] Giraldo L., Erto A., Moreno-Pirajan J.C., [Magnetite Nanoparticles for Removal of Heavy Metals From Aqueous Solutions: Synthesis and Characterization](#), *Adsorption*, **19**: 465–474 (2013).
- [38] Farhadi Sh., Sohrabi M.R., Motiee F., Davallo M., [Organophosphorus Diazinon Pesticide Removing from Aqueous Solution by Zero-Valent Iron Supported on Biopolymer Chitosan: RSM Optimization Methodology](#), *Journal of Polymers and the Environment*, **29**: 103–120 (2021).

- [39] Araujo C.S.T., Almeida I.L.S., Rezende H.C., Marcionilio S.M.L.O., Leon J.J.L., de Matos T.N., Elucidation of Mechanism Involved in Adsorption of Pb(II) onto lobeira Fruit (*Solanum lycocarpum*) Using Langmuir, Freundlich and Temkin Isotherms, *Microchemical Journal*, **137**: 348-354 (2018).
- [40] Mondal S., Kumar Majumder S., Honeycomb-Like Porous Activated Carbon for Efficient Copper (II) Adsorption Synthesized from Natural Source: Kinetic Study and Equilibrium Isotherm Analysis, *Journal of Environmental Chemical Engineering*, **7**: 103236 (2019).
- [41] Amiri S., Sohrabi M.R., Motiee F., Optimization Removal of the Ceftriaxone Drug from Aqueous Media with Novel Zero-Valent Iron Supported on Doped Strontium Hexaferrite Nanoparticles by Response Surface Methodology, *ChemistrySelect*, **5**: 5831–5840 (2020).
- [42] Toutounchi S., Shariati S., Mahanpoor K., Synthesis of Nano-Sized Magnetite Mesoporous Carbon for Removal of Reactive Yellow Dye From Aqueous Solutions, *Applied Organometallic Chemistry*, **33**: e5046 (2019).
- [43] Piccin J.S., Dotto G.L., Pinto A.A., Adsorption Isotherms and Thermochemical Data of FD&C Red N° 40 Binding by Chitosan, *Brazilian Journal of Chemical Engineering*, **28**: 295-304 (2011).
- [44] Mahdavi S., Amini N., The Role of Bare and Modified Nano Nickel Oxide as Efficient Adsorbents for the Removal of Cd²⁺, Cu²⁺, and Ni²⁺ from Aqueous Solution, *Environmental Earth Sciences*, **75**: 1468 (2016).
- [45] Ali F., Ali N., Bibi I., Said A., Nawaz Sh., Ali Z., Salman S.M., Iqbal H.M.N., Bilal M., Adsorption Isotherm, Kinetics and Thermodynamic of Acid Blue and Basic Blue Dyes onto Activated Charcoal, *Case Studies in Chemical and Environmental Engineering*, **2**: 100040 (2020).
- [46] Seyedi M.S., Sohrabi M.R., Motiee F., Mortazavinik S., Removal of Acid Red 33 from Aqueous Solution Using Nanoscale Zero-Valent Iron Supported on Activated Carbon: Kinetic, Isotherm, Thermodynamic Studies, *Iranian Journal of Chemistry and Chemical Engineering (IJCCE)*, **41**: 821-831 (2022).
- [47] Abdel-Gawad S.A., Abd El-Aziz H.M., Removal of Pharmaceuticals From Aqueous Medium Using Entrapped Activated Carbon in Alginate, *Air, Soil and Water Research*, **12**: 1-7 (2019).
- [48] Zhao X., Zhao Y., Zheng M., Liu S., Xue W., Du G., Wang T., Gao X., Wang K., Hu J., Gao Z., Huang H., Efficient Separation of Vitamins Mixture in Aqueous Solution Using a Stable Zirconium-Based Metal-Organic Framework, *Journal of Colloid and Interface Science*, **555**: 714–721 (2019).
- [49] Datta D., Sah S., Rawat N., Kumar R., Application of Magnetically Activated Carbon for the Separation of Nicotinic Acid from Aqueous Solution, *J. Chem. Eng. Data*, **62**: 712-719 (2017).